Supplementary data

Physicochemical characterization of liposomes

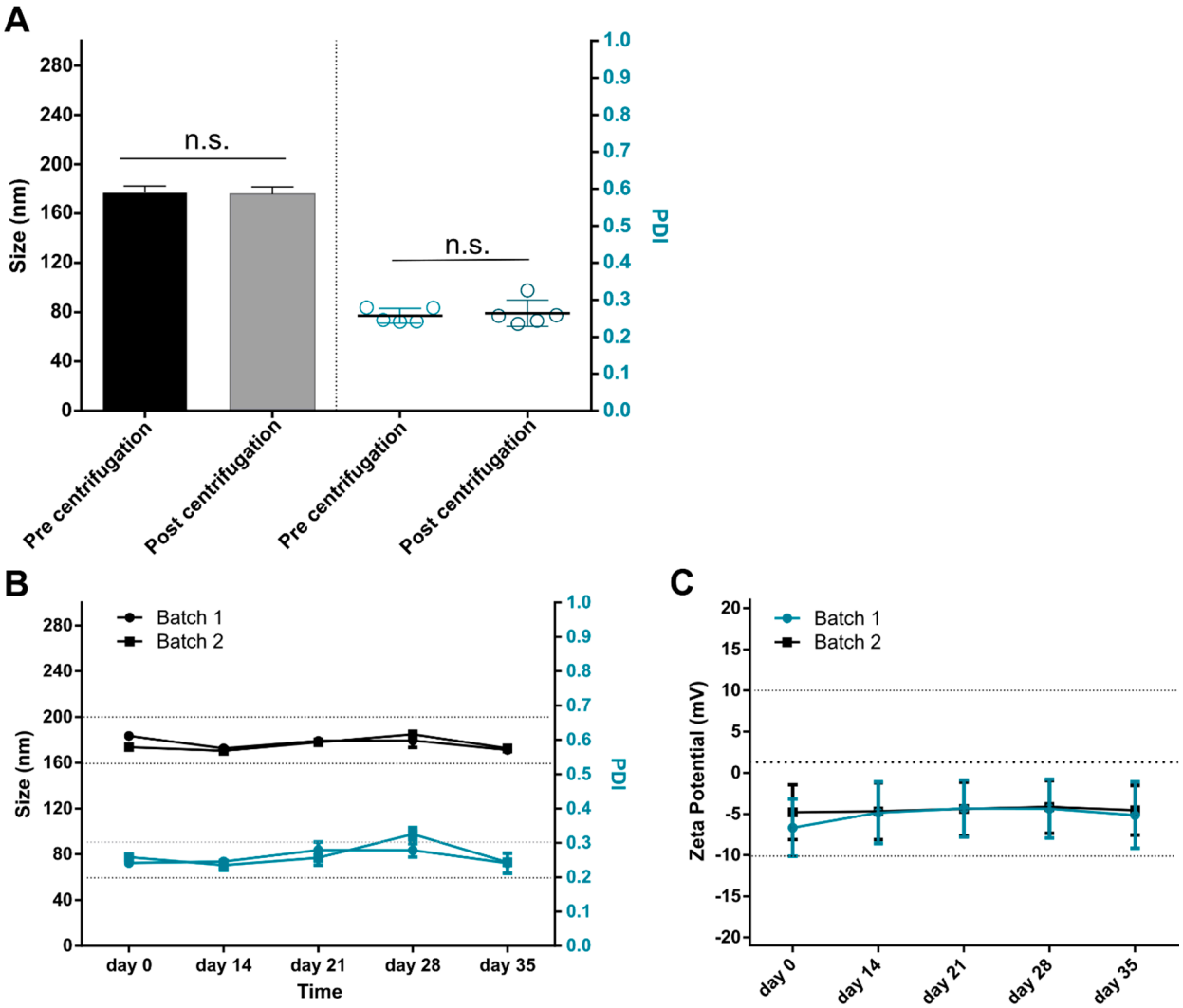

Supplementary Figure S1 | Stability of liposomes after centrifugation and shelf life. (A) Size and corresponding polydispersity index (PDI) of liposomes prior to and post centrifugation. Size, PDI and zeta-potential (B) of liposomes is monitored over time using Dynamic Light Scattering. The graphs show a stable liposome formulation that is able to conserve its physicochemical properties for at least one month (35 days).

Liposome coupling to microbubbles – flow cytometry gating strategy

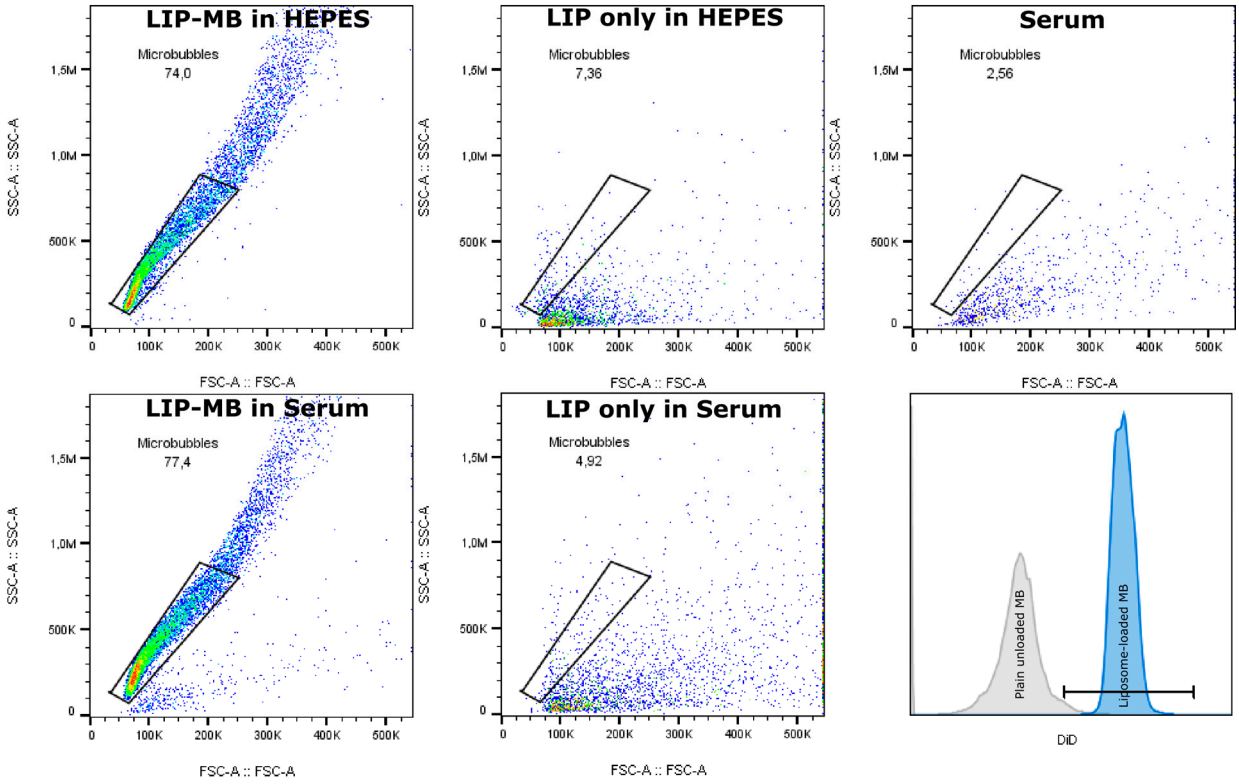

Supplementary Figure S2 | Flow cytometry gating for microbubbles. Microbubble loading can be determined accurately using flow cytometry. This technique allows detection of liposome-loading on every single microbubble and is therefore an ideal way to quantitatively estimate the liposome loading of the complete population in function of histograms or MFI. The graphs display the microbubble gating in different media HEPES and serum in both the presence and absence of microbubbles. For DiD-labelled liposomes, microbubble loading was detected in the APC-channel after fluorophore excitation by a 633 nm laser.

Liposome-loading of microbubbles

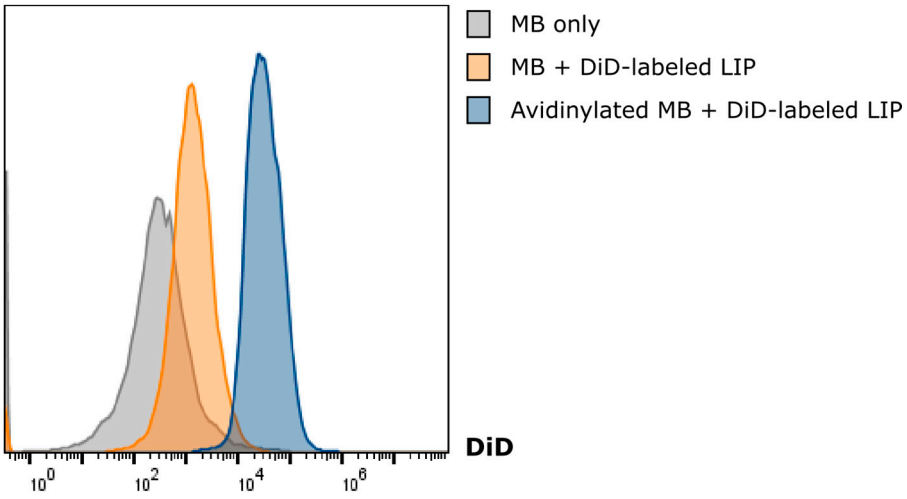

Supplementary Figure S3 | Comparison of liposome loading of microbubbles with and without avidinylation. Flow cytometry was used to measure the mean fluorescence intensity (MFI) of the different microbubble samples to quantify binding of biotinylated, DiD labelled liposomes to the microbubble surface. The graph compares MFI's of blank microbubbles (e.g. without addition of DiD liposomes, grey histogram), microbubbles incubated with DiD liposomes without avidinylation of the microbubbles (orange histogram) and microbubble incubated with DiD liposomes after avidinylation of the microbubbles (blue histogram).

Visual CIA scoring

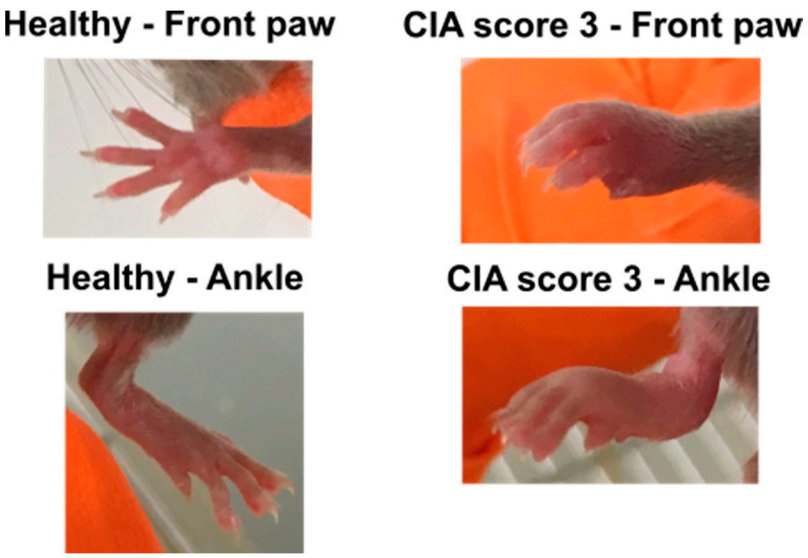

Supplementary Figure S4 | Swelling and erythema in paws with a CIA score 3 compared to healthy paws.

VEVO Liposome influx

Supplementary Figure S5 | Microbubble influx in knee synovium. The microbubble influx in a healthy (pre-CIA) (left) and CIA-induced (right) mouse, measured by contrast ultrasound and plotted in a contrast mean power graph (a.u.), indicates a detectable enhancement of contrast when microbubbles rush in the joint vasculature.

Liposome accumulation – absolute radiance values of original formulation

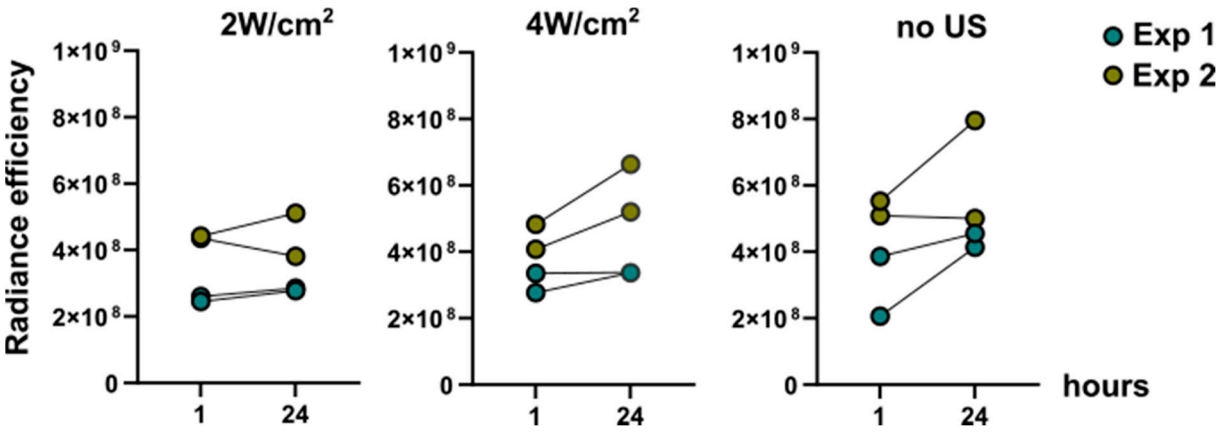

Supplementary Figure S6 | Absolute quantification in radiance at 1 and 24 hours post injection. (A) The absolute value of the liposome radiance in CIA score 3 US-treated knees, and all score 3 joints in no-US treated mice, at respectively 1 and 24 hours (connected with line) after liposome-loaded MB injection.

Liposome-loaded microbubbles – optimization study

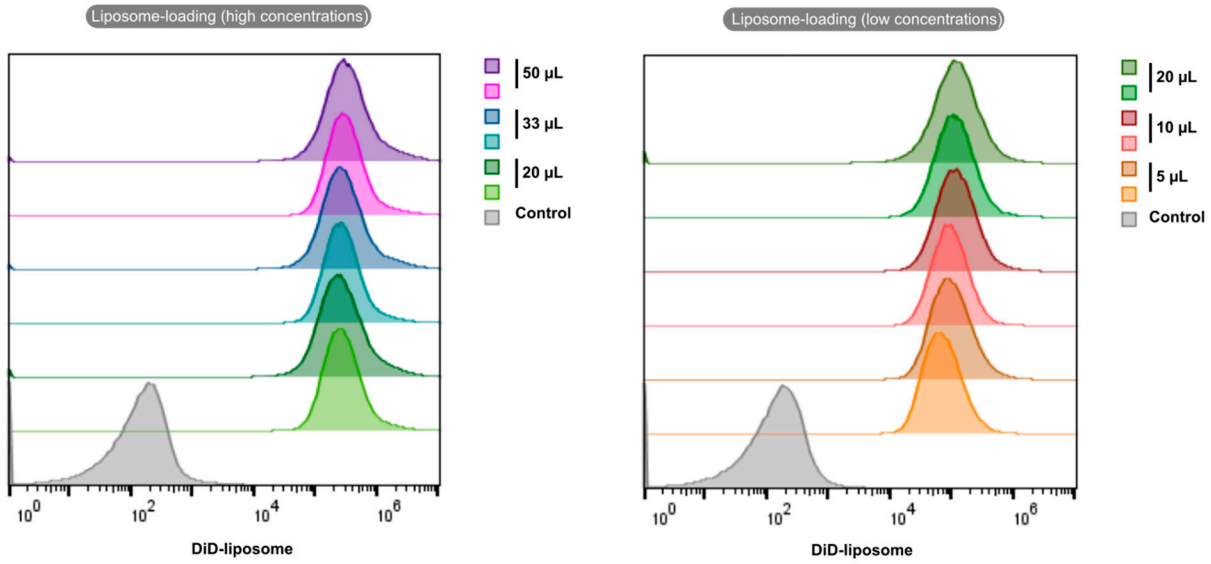

Supplementary Figure S7 | Liposome-loaded microbubbles optimization. The microbubble shell fluorescence by liposome attachment was first determined flow cytometry. The obtained histograms for 5 µL to 50 µL per 500 µL MB are shown.

Liposome accumulation – absolute radiance values of optimized formulation

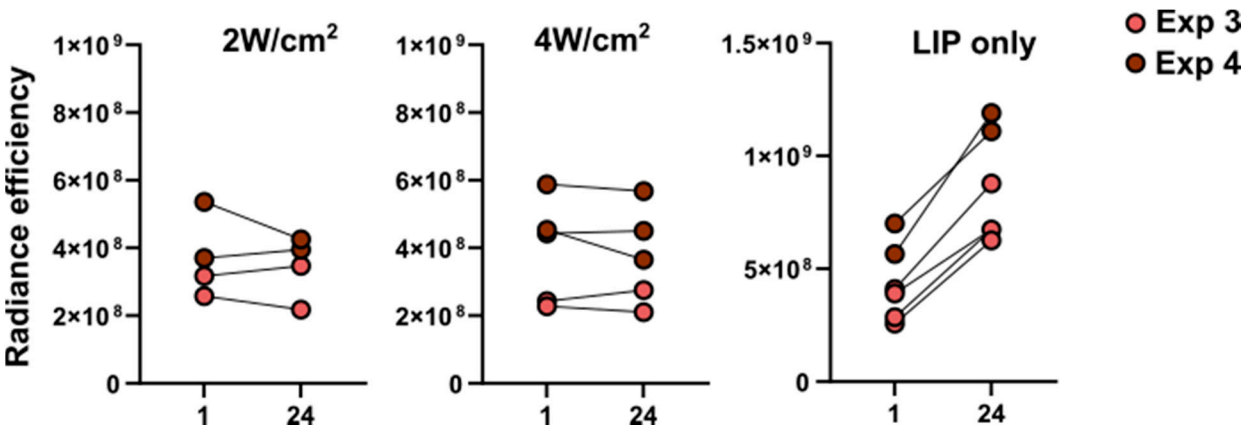

Supplementary Figure S8 | Absolute quantification in radiance in joints at 1 and 24 hours post injection. (A) The absolute value of the liposome radiance in CIA score 3 US-treated knees and, all score 3 joints in liposome (LIP) only mice, at respectively 1 and 24 hours (connected with line) after liposome-loaded MB or LIP injection.